Computation of Phase and Chemical Equilibria in Flue-Gas/Water Systems

Michael Luckas and Klaus Lucas
Dept. of Applied Thermodynamics, University of Duisburg, D-47048 Duisburg, Germany

Hans Roth
Inst. of Environmental Technology and Analysis, IUTA, D-47229 Duisburg, Germany

The phase and chemical equilibria of flue-gas/water systems containing sour gases such as HCl, HF, SO_2, SO_3, NO_x and volatile heavy metal compounds such as Hg, $HgCl_2$, and SeO_2 are calculated from thermodynamic standard data using the Gibbs free energy minimization method. The Pitzer/Debye/Hückel equation is used for the activity coefficients of the ions in the aqueous solution. The inhibition of certain oxidation reactions is considered by a proper formulation of the atom matrix. The comparison of the calculated equilibrium values to experimental data from a coal-fired power plant show that concentrations of most pollutants at the outlet of the absorbers are close to the equilibrium values of one single theoretical stage. The extension of the Gibbs free energy minimization to multistage countercurrent absorbers gives the concentration profiles of various components.

Introduction

Flue-gas cleaning using acid or alkaline aqueous solutions as solvent is characterized by a large number of components and possible reactions. Main components in the flue gas of fossil power plants or waste incineration plants are sour gases such as HCl, HF, SO_2, SO_3, NO_x, and volatile heavy metal compounds such as Hg, $HgCl_2$, and SeO_2. In aqueous solutions these components dissolve in molecular as well as in ionic form. Due to the low solubility, some reaction products precipitate as solids.

The thermodynamic modeling of flue-gas/water systems therefore implies the computation of simultaneous phase and chemical equilibria including the formation of ions and the estimation of activity coefficients in the solution. A powerful algorithm to perform such equilibrium calculations is the minimization of the Gibbs free energy (Gautam and Seider, 1979; White and Seider, 1981; Smith and Missen, 1982; Gautam and Wareck, 1986). Thermophysical properties needed are the vapor pressures of the pure components, the heats of formation, the entropies and the heat capacities of all species in well-defined standard states, for example, the pure ideal gas, the pure liquid or solid, and the hypothetical ideal 1-molal aqueous solution. A large number of these data is compiled in the literature and in special computer-based data banks. The partial molal heat capacity of the ions can be estimated by the method of Criss and Cobble (1964). Since the ionic strength typically is low, a Debye/Hückel equation, modified by Pitzer (1980), is used for the activity coefficients. Chemical *a priori* knowledge concerning the inhibition of certain oxidation reactions can be introduced by a proper formulation of the atom matrix.

The reliability of the standard data and the activity coefficient model is tested by a comparison with experimental vapor pressure and solubility data for the binary systems H_2O-HCl, H_2O-SO_2, H_2O-Hg, and H_2O-$HgCl_2$. Experimental data from the flue-gas cleaning of a coal-fired power plant shows that the chosen thermodynamic model allows the prediction of equilibrium behavior of the pollutants in the flue-gas/water system with sufficient accuracy. Particularly studied is the absorption of mercury and mercury(II) chloride from a flue gas containing HCl, SO_2, and solid carbon.

Minimization of the Gibbs Free Energy

The thermodynamic equilibrium at constant temperature T and pressure p is given by the minimum of the Gibbs free energy G:

Correspondence concerning this article should be addressed to M. Luckas.

$$G(T,p,\{N_k\}) = \sum_p^P \sum_i^C N_i^{(p)} \mu_i^{(p)} = \min \qquad (1)$$

where $\mu_i^{(p)}(T,p,\{x_k^{(p)}\})$ is the chemical potential of species i in phase p, $N_i^{(p)}$ is the number of moles of species i in phase p, and C is the number of chemical species. The number of phases P and their compositions $\{x_k^{(p)}\}$ are unknown at equilibrium. The Gibbs free energy is minimized subject to the atom balances:

$$\sum_p^P \sum_i^C N_i^{(p)} a_{ik} = A_k, \quad k=1, E \qquad (2)$$

and the electroneutrality in the liquid phase (suffix l):

$$\sum_i^C N_i^l z_i = 0. \qquad (3)$$

In Eq. 2 a_{ik} is the number of atoms of element k in species i, A_k is the total number of atoms of element k in the system, and E is the number of elements. In Eq. 3 z_i denotes the electric charge of species i.

Using Lagrange multipliers λ_k, the unconstrained objective function:

$$L(T,p,\{N_k\},\{\lambda_k\}) = \sum_p^P \sum_i^C N_i^{(p)} \mu_i^{(p)} + \sum_k^E \lambda_k \left(\sum_p^P \sum_i^C N_i^{(p)} a_{ik} - A_k \right) + \lambda_e \sum_i^C N_i^{(l)} z_i \qquad (4)$$

is minimized using:

$$\frac{\partial L}{\partial N_i^{(p)}} = 0, \quad i=1, C; \quad p=1, P \qquad (5)$$

$$\frac{\partial L}{\partial \lambda_k} = 0, \quad k=1, E \qquad (6)$$

$$\frac{\partial L}{\partial \lambda_e} = 0 \qquad (7)$$

For a system consisting of one gas phase (suffix g), one liquid phase, and any number of pure solids (suffix s), Eqs. 5-7 give:

gas phase:

$$\mu_i^g + \sum_k^E \lambda_k a_{ik} = 0, \quad i=1, C \qquad (8)$$

liquid phase:

$$\mu_i^l + \sum_k^E \lambda_k a_{ik} + \lambda_e z_i = 0, \quad i=1, C \qquad (9)$$

solid phases:

$$g_{0i}^s + \sum_k^E \lambda_k a_{ik} = 0, \quad i=1, S \qquad (10)$$

$$\sum_i^C (N_i^l + N_i^g + N_i^s) a_{ik} = A_k, \quad k=1, E \qquad (11)$$

$$\sum_i^C N_i^l z_i = 0 \qquad (12)$$

In Eq. 10 the number of solid phases S is restricted to $S \leq E$.

Computation of Chemical Potentials from Reference Data

Equations 8-12 represent a set of $2C+S+E+1$ equations to calculate the $2C+S$ unknown mole numbers and the $E+1$ Lagrange multipliers. To solve these equations, the chemical potentials $\mu_i^{(p)}$ in the different phases have to be expressed as a function of the state variables, that is, T, p, and $\{N_k\}$. Using the chemical potential of the pure components (index oi) in the ideal gas state (suffix ig) at the given temperature and the standard pressure $p_0 = 0.1$ MPa as reference, the chemical potentials in the gaseous and liquid mixture are given by:

$$\mu_i^g(T,p,\{x_k^g\}) = g_{0i}^{0,\mathrm{ig}}(T,p^0) + RT \ln\,(x_i^g \phi_i^g p/p^0), \qquad (13)$$

$$\mu_i^l(T,p,\{x_k^l\}) = g_{0i}^{0,\mathrm{ig}}(T,p^0) + RT \ln\,(x_i^l \gamma_i^0) + RT \ln\,(\phi_{s_{oi}} p_{s_{oi}}/p^0) + \int_{p_{s_{oi}}}^{p} v_{0i}^l dp \qquad (14)$$

For supercritical species and ions the hypothetical ideal solution at unit molality $m^* = 1$ mol·kg^{-1} (suffix *) is used as reference state for the liquid phase:

$$\mu_i^l(T,p,\{m_k^l\}) = \mu_i^{0,*}(T,p^0,m_i^*) + RT \ln\left(\frac{m_i}{m_i^*}\gamma_i^*\right) + \int_{p^0}^{p} v_i^* dp \qquad (15)$$

$$\mu_{i_+}^l(T,p,\{m_k^l\}) = \mu_{i_+}^{0,*}(T,p^0,m_{i_+}^*) + RT \ln\left(\frac{m_{i_+}}{m_{i_+}^*}\gamma_{i_+}^*\right) + \int_{p^0}^{p} v_{i_+}^* dp \qquad (16a)$$

$$\mu_{i_-}^l(T,p,\{m_k^l\}) = \mu_{i_-}^{0,*}(T,p^0,m_{i_-}^*) + RT \ln\left(\frac{m_{i_-}}{m_{i_-}^*}\gamma_{i_-}^*\right) + \int_{p^0}^{p} v_{i_-}^* dp \qquad (16b)$$

In the above, x_i^g and x_i^l are the mole fractions in the gas and the liquid, $p_{s_{0i}}$ is the vapor pressure of the pure component, v_{0i}^l is the pure component liquid volume, ϕ_i^g is the fugacity coefficient of component i in the gas mixture, $\phi_{s_{0i}}$ is the fugacity coefficient of pure saturated vapor at T and $p_{s_{0i}}$, and γ_i^0, γ_i^*, $\gamma_{i_+}^*$, $\gamma_{i_-}^*$ are the activity coefficients of the molecular and ionic species in the liquid mixture. Due to the different reference states, that is, the pure liquid and the infinite dilute solution, the limiting behavior of the activity coefficients is:

$$\gamma_i^0(x_i=1)=1 \tag{17}$$

$$\gamma_i^*(x_0=1)=\gamma_{i_+}^*(x_0=1)=\gamma_{i_-}^*(x_0=1)=1 \tag{18}$$

where x_0 is the mole fraction of the solvent.

It should be noted that the use of the ideal gas and the ideal 1-molal solution as reference is equivalent to the use of Henry's coefficient since:

$$H_i(T,p^0,m_i^*)=\frac{p^0}{m_i^*}\exp\left(\left(\mu_i^{0,*}-g_{0i}^{0,\mathrm{ig}}\right)/RT\right) \tag{19}$$

Using specific heat capacities at constant pressure, the chemical potentials at the reference state, that is, $g_{0i}^{0,\mathrm{ig}}\ (T,p^0)$, $\mu_i^{0,*}\ (T,p^0,m_i{*})$, $\mu_{i_+}^{0,*}\ (T,p^0,m_{i_+}^*)$, and $\mu_{i_-}^{0,*}\ (T,p^0,m_{i_-}^*)$, can be calculated at any temperature from the tabulated values of the standard enthalpy of formation $\Delta h_f^0(T^0=298.15\ \mathrm{K},\ p^0=0.1\ \mathrm{MPa})$ and the standard Gibbs energy of formation $\Delta g_f^0(T^0=298.15\ \mathrm{K},\ p^0=0.1\ \mathrm{MPa})$.

Since the number of moles of the species appear both in linear and logarithmic form, the given set of equations is nonlinear and a suitable iterative algorithm like, for example, Newton-Raphson must be used to solve the problem. In typical flue-gas calculations it is difficult to give proper guesses for all mole numbers. Often the decade of certain species in the equilibrium state is unknown. To achieve good convergence, even for poor guesses, it is essential in such calculations to use the logarithms of the mole numbers, that is, ln N_i, as variables instead of the mole numbers itself.

Thermodynamic Model

The above equations enable the exact calculation of any phase and chemical equilibria. Data needed therefore are (1) fundamental thermodynamic properties in well-defined standard states, which are tabulated for a large number of compounds in various data compilations, for example, Wagman et al. (1982), Bard et al. (1985), Reid et al. (1987), Knacke et al. (1991), and (2) suitable models to describe the deviations from the ideal gas and the ideal solution. The nonideality of the gas phase is considered by the fugacity coefficients ϕ_i^g and $\phi_{s_{0i}}$, while the deviations from Raoult's and Henry's law are given by the activity coefficients γ_i^0 and γ_i^*. In typical flue-gas/water systems the partial pressures of the various pollutants at equilibrium are so low, that the gas phase can be treated as an ideal gas without any loss of accuracy. The exact calculation of the liquid phase requires a theory for the excess Gibbs energy of multicomponent mixtures as, for example, the local composition models of Chen and Evans (1986) or Liu et al. (1989), considering the interaction between all molecular and ionic species. Due to the large number of species, a huge amount of experimental binary and ternary equilibrium data, including a complete speciation of the ionic species, is necessary to determine the parameters of the model. Since these data are not available and considering that most of the species in the aqueous phase are normally below 0.1 mol·kg^{-1}, the following simplifications are made in our calculations:

(i) The activity coefficients of all molecular solutes are set to unity, that is, salting-in and salting-out effects are neglected.

(ii) The activity coefficients of the ionic species are calculated by the Pitzer/Debye/Hückel equation (Pitzer, 1980):

$$\ln\gamma_i^* = -A_\phi/M_0^{1/2}\{(2z_i^2/\rho)\ln(1+\rho I_x^{1/2}) + (z_i^2 I_x^{1/2}-2I_x^{3/2})/(1+\rho I_x^{1/2})\} \tag{20}$$

with

$$I_x\equiv\frac{1}{2}\sum_i^C z_i^2 x_i \tag{21}$$

as the ionic strength, and ρ as adjustable parameter. The Debye/Hückel parameter A_ϕ for aqueous electrolyte systems in the range of 0°C $\leq t\leq$ 350°C is calculated by (Chen, 1982):

$$\begin{aligned}A_\phi= &-61.44534\exp\{(T-273.15)/273.15\}\\ &+2.864468[\exp\{(T-273.15)/273.15\}]^2\\ &+183.5379\ln(T/273.15)-0.6820223(T-273.15)\\ &+0.0007875695[T^2-(273.15)^2]+58.95788(273.15/T)\end{aligned} \tag{22}$$

Furthermore, the pressure dependence of the chemical potential in the liquid phase, that is, the Poynting factor, is neglected in Eqs. 14–16.

Binary Systems

To check the reliability of the experimental basis data, especially the enthalpy and Gibbs energy of formation as well as the heat capacities, and to test the activity coefficient model, the equilibria of the most important binary systems have been calculated and compared to experimental data. In Tables 1 and 2, the Gibbs energies of formation, the enthalpies of formation, and the heat capacities used in all our calculations are given for the most important species. Vapor pressures and heat capacities in the ideal gas are taken from Reid et al. (1987). The partial molal heat capacities of the ions in the ideal aqueous solution at unit molality are estimated by the method of Criss and Cobble (1964).

Figure 1 shows the influence of parameter ρ in the Pitzer/Debye/Hückel equation. Since HCl is the strongest dissociating species in the flue-gas cleaning process, and therefore may exceed the limit of the Pitzer equation, ρ was adjusted for this component to vapor pressure data (Fritz and Fuget, 1956). As shown in Table 3, in the range of $0\leq m_{\mathrm{HCl}}\leq 0.5$ mol·kg^{-1}, $293.15\leq T\leq 323.15$ K, a value of $\rho_{\mathrm{HCl}}=29$ gives a satisfying correlation of the data. For all other ionic species, a value of 14.9 originally given by Pitzer is used. It is important to mention that the use of different values for the parameter ρ is inconsistent with the derivation of the Pitzer/Debye/Hückel equation. The change of ρ for HCl-H_2O is purely empirical but leads to reasonable results in dilute solutions. A more consistent representation of the activity coefficients in multicomponent electrolyte solutions would require a larger number of adjustable binary parameters which often cannot be determined due to the lack of experimental data.

Tables 4–6 show a comparison of experimental and calculated data for the systems SO_2-H_2O and Hg-H_2O. As indicated in Table 1, the partial molal heat capacities of sulfur dioxide and mercury in the ideal aqueous solution are adjusted to the vapor pressure and solubility data in Tables 5 and 6. For both systems, the model gives a good representation of the data.

Table 1. Thermodynamic Data at $T^0 = 298.15$ K, $p^0 = 0.1$ MPa (Wagman et al., 1982; Bard et al., 1985)

Species	$\Delta g^{0,ig}_{f_{0i}}$ kJ·mol^{-1}	$\Delta h^{0,ig}_{f_{0i}}$ kJ·mol^{-1}	$\Delta\mu^{0,*}_{f_i}$ kJ·mol^{-1}	$\Delta h^{0,*}_{f_i}$ kJ·mol^{-1}	$c^{0,*}_{p_i}$ J·mol^{-1}K^{-1}
H_2O(g)	−228.572	−241.818			
HCl(g)	−95.299	−92.307			
HF(g)	−273.2	−271.1			
HF(aq)			−296.82	−320.08	—
H^+(aq)			0	0	*
OH^-(aq)			−157.244	−229.994	*
Cl^-(aq)			−131.228	−167.159	*
F^-(aq)			−278.79	−332.63	*
SO_2(g)	−300.194	−296.830			
SO_2(aq)			−300.676	−322.980	150.0 (adjusted)
HSO_3^-(aq)			−527.73	−626.22	*
SO_3^{2-}(aq)			−486.5	−635.5	*
Hg(g)	31.820	61.317			
Hg(aq)			37.20	19.5	200.0 (adjusted)
$HgCl_2$(g)	−141.8	−143.1			
$HgCl_2$(aq)			−173.2	−216.3	−26.3 (adjusted)
$Hg(OH)_2$(aq)			−274.8	−355.2	—
$HgOH^+$(aq)			−52.3	−84.5	*
$HgCl^+$(aq)			−5.4	−18.8	*
$HgCl_3^-$(aq)			−309.1	−388.7	*
$HgCl_4^{2-}$(aq)			−446.8	−554.0	*

*Estimated by the method of Criss and Cobble (1964).

In coal-fired power plants, mercury mostly is emitted in its atomic form, while in waste incineration plants it is emitted as mercury(II) chloride, $HgCl_2$. In Table 7 the calculated solubility of solid $HgCl_2$ in water at 298.15 K is shown. In pure water, mercury(II) chloride is almost completely dissolved in its molecular form. Compared to Hg, Table 6, the solubility in water is extremely high, while the vapor pressure is much lower. The calculated solubility differs from the experimental value by a factor of ~2.4. The reason for this relative large deviation will probably arise from the assumption of an ideal dilute solution for the dissolved mercury chloride, that is, $\overset{*}{\gamma}_{HgCl_2} = 1$, which is generally not allowed at the given concentration. Other reasons may be inaccuracies in the used standard data or the formation of dimers at infinite dilution. In the flue gas of a waste incineration plant, the concentration of gaseous $HgCl_2$ is in the ppm range, and the concentration in the aqueous solution is up to five decades below the saturation concentration, calculated in Table 7. Therefore, it can be assumed that

Table 2. Thermodynamic Data of Pure Liquids and Solids at $T^0 = 298.15$ K, $p^0 = 0.1$ MPa (Wagman et al., 1982; Knacke et al., 1991)

Species	$\Delta g^0_{f_{0i}}$ kJ·mol^{-1}	$\Delta h^0_{f_{0i}}$ kJ·mol^{-1}	$c^0_{p_{0i}}$ J·mol^{-1}·K^{-1}
Hg(l)	0	0	27.983
$HgCl_2$(s)	−178.6	−224.3	73.93
Se(s)	0	0	25.363
$CaSO_4 \cdot 2H_2O$(s)	−1,797.28	−2,022.63	186.02
CaF_2(s)	−1,167.3	−1,219.6	67.03

Table 3. Partial Vapor Pressure of HCl over Aqueous Solutions

T K	m_{HCl} mol·kg^{-1}	$\overset{*}{\gamma}_{\pm}$(Cal.)	p_{HCl}(Cal.) kPa	p_{HCl}(Exp.) kPa
293.15	0.01	0.911	0.253×10^{-8}	0.245×10^{-8}
	0.05	0.843	0.541×10^{-7}	0.517×10^{-7}
	0.10	0.807	0.198×10^{-6}	0.191×10^{-6}
	0.20	0.769	0.720×10^{-6}	0.704×10^{-6}
	0.50	0.716	0.391×10^{-5}	0.435×10^{-5}
323.15	0.01	0.906	0.458×10^{-7}	0.447×10^{-7}
	0.05	0.835	0.971×10^{-6}	0.933×10^{-6}
	0.10	0.797	0.354×10^{-5}	0.336×10^{-5}
	0.20	0.757	0.128×10^{-4}	0.125×10^{-4}
	0.50	0.702	0.688×10^{-4}	0.721×10^{-4}

Experimental data from Fritz and Fuget (1956).

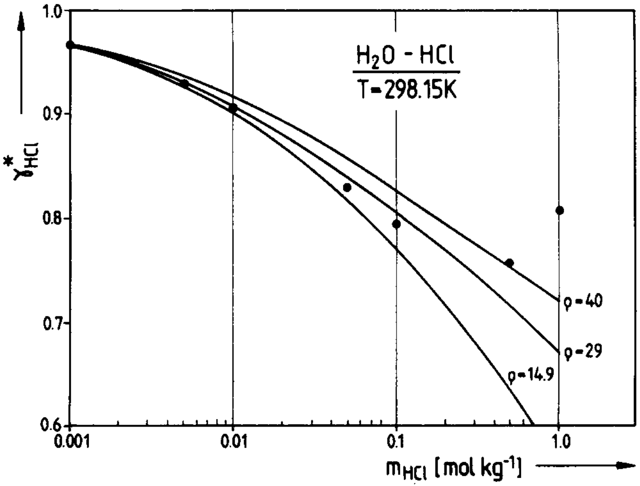

Figure 1. Mean ion-activity coefficient of HCl vs. molality.

●, experimental data from Harned and Owen (1985); —, Eq. 20.

Table 4. Degree of Dissociation and Partial Vapor Pressures of SO_2 over Aqueous Solutions at 298.15 K

m_{SO_2} mol·kg^{-1}	α(Cal.)	α(Exp.)	p_{SO_2}(Cal.) kPa	p_{SO_2}(Exp.) kPa
0.0271	0.583	0.524	0.933	1.05
0.0854	0.411	0.363	4.14	4.56
0.1663	0.326	0.285	9.24	9.84
0.2873	0.266	0.230	17.4	18.1
0.5014	0.215	0.184	32.4	33.7

Experimental data from Johnstone and Leppla (1934).

Table 5. Temperature Dependence of Partial Vapor Pressures of SO_2 over Aqueous Solutions

T °C	m_{SO_2} mol·kg^{-1}	α(Cal.)	p_{SO_2}(Cal.) kPa	p_{SO_2}(Exp.) kPa
30	0.0921	0.382	5.56	5.47
30	0.501	0.203	39.1	41.1
50	0.0921	0.308	11.4	11.5
50	0.501	0.158	75.4	77.9
70	0.0921	0.237	20.4	20.3
80	0.0921	0.206	26.0	25.2

Experimental data from Rabe and Harris (1963).

if the deviation arises from the activity coefficient, at lower concentrations the solubility of $HgCl_2$ will be calculated more accurately.

Results for a Real Flue Gas

A comparison of our model to experimental data of well-defined multicomponent systems, such as, for example, N_2-SO_2-HCl-H_2O-Hg-$HgCl_2$, is not possible, since to our knowledge such data actually do not exist. Therefore, we compare our calculations with measurements from a real flue-gas cleaning of a coal-fired power plant (Gutberlet, 1984). Experimental mean mole fractions of the gaseous pollutants, related to the dry flue gas, are:

HCl: 0.12×10^{-3} HF: 0.90×10^{-5}

SO_2: 0.70×10^{-3} SO_3: 0.56×10^{-5}

NO: 0.60×10^{-3} NO_2: 0.21×10^{-4}

Hg: 0.16×10^{-8} SeO_2: 0.22×10^{-7}

Table 7. Solubility of Solid Mercury(II) Chloride in Aqueous Solution at $T=298.15$ K, $p=0.1$ MPa

	m_i/mol·kg^{-1}	γ_i^*	p_i/kPa
$HgCl_2$	0.1132	1	0.3572×10^{-4}
Hg	0.0	1	0.0
$Hg(OH)_2$	0.3511×10^{-4}	1	
$HgCl^+$	0.2503×10^{-3}	0.980	
$HgCl_3^-$	0.1376×10^{-3}	0.980	
$HgOH^+$	0.9141×10^{-6}	0.980	
$HgCl_4^{2-}$	0.3601×10^{-6}	0.921	
Hg^{2+}	0.2573×10^{-6}	0.921	
Hg_2^{2+}	0.0	0.921	
Cl^-	0.1846×10^{-3}	0.980	
H^+	0.7114×10^{-4}	0.980	
OH^-	0.1479×10^{-9}	0.980	
Σ Hg:	0.114 mol·kg^{-1}		
Exp:	0.269 ± 0.003 mol·kg^{-1} (Clever et al., 1985)		
pH:	4.2		

The wet part of the flue-gas cleaning plant consists of a HCl-scrubber, where the flue-gas is quenched from 140°C to 50±3°C, and a desulfurization plant using an aqueous suspension of CaO as solvent to produce gypsum. For both absorbers, equilibrium calculations have been carried out and compared to experimental measurements from the plant. The results are shown in Table 8. Considering the fact that the experimental data are taken from real, nonequilibrium multistage countercurrent absorbers, the agreement with the calculated equilibrium data is surprisingly good. Remarkable deviations are only found for Hg and Se. The relative high absorption of Hg measured in the plant results from the fact that mercury to some extent is adsorbed on small dust particles, passing the electric filter and subsequently washed out in the first absorber. The gaseous SeO_2 is reduced to Se, which precipitates as solid. The reason for the incomplete reduction and deposition in the plant is unclear.

The Gibbs free energy minimization algorithm can easily be extended to multistage countercurrent processes (Gautam and Wareck, 1986). Figure 2 shows the simulation results for the HCl absorber assuming five equilibrium stages. It can be seen that an increase of the number of stages does not increase the absorption of NO_x, Hg, and SO_2. HCl is absorbed to 99% at the first equilibrium stage and is completely washed out at the second stage. As shown in Figure 2, the absorption of HF depends strongly on the number of stages of the HCl scrubber. Hydrogen fluoride is absorbed in fresh water at the upper part of the absorber and subsequently partly desorbed at the lower

Table 6. Solubility of Mercury in Aqueous Solutions at $p=0.1$ MPa

T K	m_i(Cal.) mol·kg^{-1}	m_i(Exp.) mol·kg^{-1}	p_i(Cal.) kPa	p_i(Exp.) kPa
273.15	0.160×10^{-6}	0.136×10^{-6}	0.276×10^{-4}	0.267×10^{-4}
293.15	0.267×10^{-6}	0.246×10^{-6}	0.175×10^{-3}	0.169×10^{-3}
298.15	0.304×10^{-6}	0.303×10^{-6}	0.266×10^{-3}	0.258×10^{-3}
313.15	0.454×10^{-6}	0.442×10^{-6}	0.870×10^{-3}	0.840×10^{-3}
333.15	0.785×10^{-6}	0.787×10^{-6}	0.356×10^{-2}	0.345×10^{-2}
353.15	0.137×10^{-5}	0.138×10^{-5}	0.124×10^{-1}	0.120×10^{-1}
368.15	0.208×10^{-5}	0.210×10^{-5}	0.288×10^{-1}	0.281×10^{-1}

Experimental data from Clever et al. (1985).

Table 8. Degree of Absorption of the HCl and the SO_2 Absorber (Experimental Data from Gutberlet, 1984).

	HCl Absorber		SO_2 Absorber		Σ	
Species	Cal.	Exp.	Cal.	Exp.	Cal.	Exp.
HCl	0.99	~0.90	0.01	~0.10	1.0	~1.0
HF	0.36	~0.50	0.64†	~0.50†	1.0	~1.0
SO_2	0.03	~0.07	0.96*	~0.89*	1.0	~0.96
SO_3	1.0	~1.0	—	—	1.0	~1.0
NO_x	0	0	0.02	~0.01	0.02	~0.01
Hg	0	~0.20	0	~0.03	0	~0.23
SeO_2**	1.0	~0.50	—	~0.01	1.0	~0.51

*Precipitated as gypsum.
**Precipitated as Se.
† Precipitated as CaF_2.

stages due to the absorption of the stronger acid HCl. In this way, a cycle stream of HF is generated. Nevertheless, in five equilibrium stages a complete absorption of HF can be reached. Finally, these results show that the efficiency of both absorbers for most of the components is nearly equal to one single theoretical equilibrium stage.

Detailed results of the equilibrium calculations for both absorbers are given in Tables 9 and 10. For the species HgS(s), HgF^+(aq), $HgSO_4$(aq), SF_6(g), Cl_2(g), NO_2^-(aq), NO_3^-(aq), Se_2(g), SeO(g), SeO_2(g), SeF_6(g), H_2SeO_3(aq), H_2SeO_4(aq), HSe^-(aq), $HSeO_3^-$(aq), $HSeO_4^-$(aq), SeO_3^{2-}(aq) and SeO_4^{2-}(aq), not given in Table 9, mole numbers less than 10^{-12} have been calculated. To prevent oxidation reactions such as, for example,

$$NO+\frac{1}{2}\,O_2\rightleftharpoons NO_2 \quad \text{or} \quad SO_2+\frac{1}{2}\,O_2\rightleftharpoons SO_3,$$

which are known to be kinetically inhibited at the given temperature, oxygen was omitted in the equilibrium calculation of the HCl absorber. For the desulfurization, oxygen is needed for the formation of gypsum. To enable this reaction and to prevent other oxidation reactions, two different species of oxygen, one reactive and one nonreactive, have been introduced in the formula matrix. The species O_2 and $CaSO_4\cdot 2H_2O$ (gypsum) contain the reactive oxygen, while all other species contain the nonreactive oxygen atom. In this way, chemical *a priori* knowledge concerning the inhibition of certain reactions can easily be introduced into the equilibrium calculation.

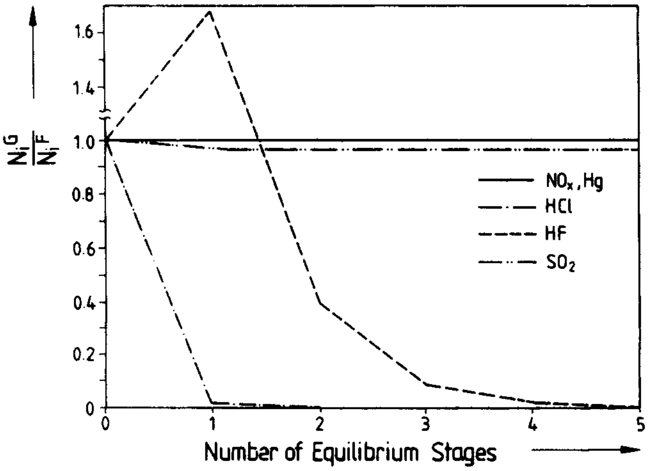

Figure 2. Individual component flows in a five-stage countercurrent absorber.

N_i^G, N_i^F: mole flow of component *i* in the gas and the feed.

Table 9. Equilibrium Results for the HCl Absorber (T = 323.15 K, p = 0.1 MPa)

	N_i^l/mol	γ_i^*	N_i^g/mol
N_2	0.0	1	1.0
H_2O	0.01220	1	0.1378
SO_2	0.7337×10^{-7}	1	0.6789×10^{-3}
SO_3	0.0	1	0.0
H_2SO_4	0.0	1	0.0
HCl	0.1464×10^{-9}	1	0.1071×10^{-5}
HF	0.3261×10^{-5}	1	0.5733×10^{-5}
NO	0.0	1	0.6210×10^{-3}
NO_2	0.0	1	0.0
Hg	0.0	1	0.1600×10^{-8}
$HgCl_2$	0.0	1	0.0
HgCl	0.0	1	0.0
HgF	0.0	1	0.0
$Hg(OH)_2$	0.0	1	0.0
SeO_2	0.0	1	0.0
Se	0.0	1	0.0
$HgCl^+$	0.0	0.595	
$HgCl_3^-$	0.0	0.595	
$HgCl_4^{2-}$	0.0	0.124	
Hg^{2+}	0.0	0.124	
Hg_2^{2+}	0.0	0.124	
$HgOH^+$	0.0	0.595	
HSO_3^-	0.2452×10^{-8}	0.595	
HSO_4^-	0.2541×10^{-4}	0.595	
SO_3^{2-}	0.0	0.124	
SO_4^{2-}	0.1233×10^{-5}	0.124	
Cl^-	0.1189×10^{-3}	0.685	
F^-	0.5412×10^{-8}	0.595	
H^+	0.1468×10^{-3}	0.685	
OH^-	0	0.595	
Se(s)	0.2200×10^{-7} mol		
Feed:	1 mol N_2, 0.15 mol H_2O, 0.7×10^{-3} mol SO_2, 0.56×10^{-5} mol SO_3, 0.12×10^{-3} mol HCl, 0.9×10^{-5} mol HF, 0.6×10^{-3} mol NO, 0.21×10^{-4} mol NO_2, 0.16×10^{-8} mol Hg, 0.22×10^{-7} mol SeO_2		

Table 10. Equilibrium Results for the SO_2 Absorber ($T = 323.15$ K, $p = 0.1$ MPa)

	N_i^l/mol	γ_i^*	N_i^g/mol
N_2	0.0	1	0.94
O_2	0.2761×10^{-7}	1	0.5966×10^{-1}
H_2O	0.3189×10^{-1}	1	0.1408
SO_2	0.0	1	0.0
SO_3	0.0	1	0.0
H_2SO_4	0.0	1	0.0
HF	0.1693×10^{-9}	1	0.1141×10^{-9}
NO	0.0	1	0.6067×10^{-3}
NO_2	0.3252×10^{-10}	1	0.4107×10^{-8}
Hg	0.0	1	0.1599×10^{-8}
HgF	0.0	1	0.0
$Hg(OH)_2$	0.0	1	0.0
HgF^+	0.0	0.765	
Hg^{2+}	0.0	0.341	
Hg_2^{2+}	0.0	0.341	
$HgOH^+$	0.0	0.765	
HSO_3^-	0.0	0.765	
HSO_4^-	0.6401×10^{-9}	0.765	
SO_3^{2-}	0.0	0.341	
SO_4^{2-}	0.7408×10^{-5}	0.341	
NO_2^-	0.4566×10^{-6}	0.765	
NO_3^-	0.1384×10^{-4}	0.765	
HNO_2	0.3491×10^{-9}	1	
F^-	0.1116×10^{-6}	0.765	
H^+	0.6735×10^{-9}	0.765	
OH^-	0.4537×10^{-10}	0.765	
Ca^{2+}	0.1461×10^{-4}	0.341	
$CaSO_4\cdot2H_2O(s)$	0.6726×10^{-3} mol		
$CaF_2(s)$	0.2794×10^{-5} mol		
Feed:	0.94 mol N_2, 0.06 mol O_2, 0.174 mol H_2O, 0.68×10^{-3} mol SO_2, 0.57×10^{-5} mol HF, 0.6×10^{-3} mol NO, 0.21×10^{-4} mol NO_2, 0.16×10^{-8} mol Hg, 0.69×10^{-3} mol CaO		

Results for the Systems H_2O-HCl-Hg-$HgCl_2$-SO_2 and H_2O-HCl-Hg-$HgCl_2$-C(s)

Table 11 shows the solubility of gaseous $HgCl_2$ in a dilute aqueous HCl solution at 323.15 K. Main Hg species in the liquid are found to be $HgCl_2$ (67%) and the $HgCl_3^-$ and $HgCl_4^{2-}$ complexes. This result corresponds quite well to experimental results (Sjöberg, 1977; Nagypál and Beck, 1982). Measurements from various flue-gas cleaning plants indicate that the highly soluble mercury(II) chloride in the wet cleaning process can be reduced to some extent by sulfur dioxide or soot particles to atomic mercury. Since mercury is nearly insoluble in the aqueous phase, this reduction decreases the efficiency of the absorption. Tables 12-13 show that in the thermodynamic equilibrium $HgCl_2$ is totally reduced to Hg by SO_2 or solid carbon. The same is true for the presence of carbon monoxide. A variation of the mole numbers of SO_2, C, CO, and HCl shows that the results in Tables 12 and 13 concerning the reduction of $HgCl_2$ are very insensitive to the concentrations of the species. The overall balances can be written as:

$$HgCl_2 + 2H_2O + SO_2 \rightleftharpoons Hg + 2Cl^- + 3H^+ + HSO_4^-,$$

$$2HgCl_2 + 2H_2O + C \rightleftharpoons 2Hg + 4Cl^- + 4H^+ + CO_2.$$

Table 11. Equilibrium Results for the System H_2O-HCl-$HgCl_2$ at $T = 323.15$ K, $p = 0.1$ MPa

	N_i^l/mol	γ_i^*	N_i^g/mol
N_2	0.0		1.0
H_2O	0.1593	1	0.1407
Hg	0.0	1	0.0
$HgCl_2$	0.1343×10^{-6}	1	0.1707×10^{-8}
HgCl	0.0	1	0.0
$Hg(OH)_2$	0.0	1	0.0
HCl	0.1371×10^{-10}	1	0.7867×10^{-8}
$HgCl^+$	0.4587×10^{-11}	0.819	
$HgCl_3^-$	0.3211×10^{-7}	0.819	
$HgCl_4^{2-}$	0.3191×10^{-7}	0.449	
Hg^{2+}	0.0	0.449	
Hg_2^{2+}	0.0	0.449	
$HgOH^+$	0.0	0.819	
Cl^-	0.1199×10^{-3}	0.844	
H^+	0.1200×10^{-3}	0.844	
OH^-	0.0	0.819	
pH: 1.45			
Feed:	1 mol N_2, 0.3 mol H_2O, 0.12×10^{-3} mol HCl, 0.2×10^{-6} mol $HgCl_2$		

Due to low mass transfer and/or reaction rates in technical flue-gas cleaning processes the reduction of the mercury(II) chloride is incomplete. Furthermore, the oxygen in the flue gas, which is omitted in the equilibrium calculations, may influence the real reduction process.

Table 12. Equilibrium Results for the System H_2O-HCl-$HgCl_2$-Hg-SO_2 at $T = 323.15$ K, $p = 0.1$ MPa

	N_i^l/mol	γ_i^*	N_i^g/mol
N_2	0.0		1.0
H_2O	0.1593	1	0.1407
SO_2	0.1403×10^{-6}	1	0.9961×10^{-4}
Hg	0.1667×10^{-10}	1	0.2000×10^{-6}
$HgCl_2$	0.0	1	0.0
HgCl	0.0	1	0.0
$Hg(OH)_2$	0.0	1	0.0
$HgSO_4$	0.0	1	—
HCl	0.0	1	0.0
$HgCl^+$	0.0	0.818	
$HgCl_3^-$	0.0	0.818	
$HgCl_4^{2-}$	0.0	0.448	
Hg^{2+}	0.0	0.448	
Hg_2^{2+}	0.0	0.448	
$HgOH^+$	0.0	0.818	
HSO_3^-	0.4484×10^{-7}	0.818	
HSO_4^-	0.1615×10^{-6}	0.818	
SO_3^{2-}	0.0	0.448	
SO_4^{2-}	0.3850×10^{-7}	0.448	
Cl^-	0.1204×10^{-3}	0.843	
H^+	0.1207×10^{-3}	0.843	
OH^-	0.0	0.818	
pH: 1.45			
$HgCl_2 + 2H_2O + SO_2 \rightleftharpoons Hg + 2Cl^- + 3H^+ + HSO_4^-$ $HSO_4^- \rightleftharpoons H^+ + SO_4^{2-}$			
Feed:	1 mol N_2, 0.3 mol H_2O, 0.1×10^{-3} mol SO_2, 0.12×10^{-3} mol HCl, 0.2×10^{-6} mol $HgCl_2$		

Table 13. Equilibrium Results for the System H_2O-HCl-$HgCl_2$-Hg-C at $T=323.15$ K, $p=0.1$ MPa

	N_i^l/mol	γ_i^*	N_i^g/mol
N_2	0.0		1.0
H_2O	0.1593	1	0.1407
CO_2	0.4483×10^{-11}	1	0.1×10^{-6}
CO	0.0		0.0
Hg	0.1667×10^{-10}	1	0.2000×10^{-6}
$HgCl_2$	0.0	1	0.0
HgCl	0.0	1	0.0
$Hg(OH)_2$	0.0	1	0.0
HCl	0.0	1	0.0
$HgCl^+$	0.0	0.819	
$HgCl_3^-$	0.0	0.819	
$HgCl_4^{2-}$	0.0	0.449	
Hg^{2+}	0.0	0.449	
Hg_2^{2+}	0.0	0.449	
$HgOH^+$	0.0	0.819	
HCO_3^-	0.0	0.819	
Cl^-	0.1204×10^{-3}	0.844	
H^+	0.1204×10^{-3}	0.844	
OH^-	0.0	0.819	
C(s)	0.9000×10^{-6}		
pH: 1.45			
$2HgCl_2+2H_2O+C\rightleftharpoons 2Hg+4Cl^-+4H^++CO_2$			
Feed:	1 mol N_2, 0.3 mol H_2O, 0.1×10^{-5} mol C, 0.12×10^{-3} mol HCl, 0.2×10^{-6} mol $HgCl_2$		

Conclusions

It is shown that the computation of phase and chemical equilibria from tabulated thermodynamic standard data, and the Pitzer/Debye/Hückel equation for the activity coefficients in combination with chemical *a priori* knowledge concerning the inhibition of certain oxidation reactions gives results for binary aqueous solutions and real multicomponent flue-gas/water systems, which compare very well with experimental data and practical experience. In particular, the equilibrium calculations give valuable information concerning the behavior of trace elements, for example, mercury and selenium in the wet flue-gas cleaning. In performing such calculations, especially for systems with a large number of possible species, we found the Gibbs minimization to be a very efficient algorithm.

To take account of multistage and nonequilibrium effects in technical absorbers or environmental systems, the equilibrium model has to be combined in a process simulator with the corresponding mass and energy balances. In combination with well-suited correlations for the heat and mass transfer, simulations provide reliable results even for rather complex thermodynamic systems.

Notation

a_{ik} = number of atoms of element k in species i
A_k = total number of atoms of element k
A_Φ = Debye/Hückel constant
c_p = molar heat capacity
C = number of species
E = number of elements
Δg_f^0 = standard Gibbs free energy of formation
G = Gibbs free energy
Δh_f^0 = standard enthalpy of formation
H_i = Henry's Law constant of species i
I = ionic strength
L = Lagrange function
m_i = molality of species i, moles per kg water
m_i^* = unit molality of species i, 1 mole per kg water
M_0 = molecular mass of water, kg per mole
N_i = number of moles of species i
p = pressure
p^0 = standard pressure of 0.1 MPa
p_{s0i} = vapor pressure of the pure species i
P = number of phases
R = universal gas constant
T = absolute temperature
v = molar volume
$x_i^{(p)}$ = mole fraction of species i in phase p
z = charge

Greek letters

γ = activity coefficient
λ = Lagrange multiplier
μ_i = chemical potential of species i
ρ = parameter in the Pitzer/Debye/Hückel Eq. 20

Superscripts

$*$ = denotes standard state as hypothetical ideal solution of unit molality and at the temperature of the system and standard pressure p^0
ig = ideal gas

Literature Cited

Bard, A. J., R. Parsons, and J. Jordan, *Standard Potentials in Aqueous Solution*, Marcel Dekker, New York (1985).

Chen, C.-C., H. I. Britt, J. F. Boston, and L. B. Evans, "Local Composition Model for Excess Gibbs Energy of Electrolyte Systems," *AIChE J.*, **28**, 588 (1982).

Chen, C.-C., and L. B. Evans, "A Local Composition Model for the Excess Gibbs Energy of Aqueous Electrolyte Systems," *AIChE J.*, **32**, 444 (1986).

Clever, H. L., S. A. Johnson, and M. E. Derrick, "The Solubility of Mercury and Some Sparingly Soluble Mercury Salts in Water and Aqueous Electrolyte Solutions," *J. Phys. Chem. Ref. Data*, **14**, 631 (1985).

Criss, C. M., and J. W. Cobble, "The Thermodynamic Properties of High Temperature Aqueous Solutions. IV. Entropies of the Ions up to 200° and the Correspondence Principle," *J. Amer. Chem. Soc.*, **86**, 5385 (1964).

Criss, C. M., and J. W. Cobble, "The Thermodynamic Properties of High Temperature Aqueous Solutions. V. The Calculation of Ionic Heat Capacities up to 200°. Entropies and Heat Capacities above 200°," *J. Amer. Chem. Soc.*, **86**, 5390 (1964).

Fritz, J. J., and C. R. Fuget, "Vapor Pressure of Aqueous Hydrogen Chloride Solutions, 0° to 50°C," *Chem. Eng. Data Ser.*, **1**, 10 (1956).

Gautam, R., and W. D. Seider, "Computation of Phase and Chemical Equilibrium: I-III," *AIChE J.*, **25**, 991 (1979).

Gautam, R., and J. S. Wareck, "Computation of Physical and Chemical Equilibria—Alternative Specifications," *Comput. Chem. Eng.*, **10**, 143 (1986).

Gutberlet, H., *Messung der Schwermetallabscheidung einer Rauchgasentschwefelungsanlage nach dem Kalkwaschverfahren*, Forschungsbericht ENV-492-D(B), VEBA Kraftwerke Ruhr AG, Gelsenkirchen, Germany (1984).

Harned, H. S., and B. B. Owen, *Physical Chemistry of Electrolyte Solutions*, Reinhold, New York (1958).

Johnstone, H. F., and P. W. Leppla, "The Solubility of Sulfur Dioxide at Low Partial Pressures. The Ionization Constant and Heat of Ionization of Sulfurous Acid," *J. Amer. Chem. Soc.*, **56**, 2233 (1934).

Knacke, O., O. Kubaschewski, and K. Hesselmann, *Thermochemical Properties of Inorganic Substances*, Vols. I and II, Springer, New York (1991).

Liu, Y., A. H. Harvey, and J. M. Prausnitz, "Thermodynamics of Concentrated Elektrolyte Solutions," *Chem. Eng. Comm.*, **77**, 43 (1989).

Nagypál, I., and M. T. Beck, "Diagrams for Complete Representation of Binary Mononuclear Complex Systems," *Talanta*, **29**, 473 (1982).

Pitzer, K. S., "Electrolytes. From Dilute Solutions to Fused Salts," *J. Amer. Chem. Soc.*, **102**, 2902 (1980).

Rabe, A. E., and J. F. Harris, "Vapor Liquid Equilibrium Data for the Binary System, Sulfur Dioxide and Water," *J. Chem. Eng. Data*, **8**, 333 (1963).

Reid, R. C., J. M. Prausnitz, and B. E. Poling, *The Properties of Gases & Liquids*, McGraw-Hill, New York (1987).

Sjöberg, S., "Metal Complexes with Mixed Ligands: 11. The Formation of Ternary Mononuclear and Polynuclear Mercury(II) Complexes in the System Hg^{2+}-Cl^--OH^-. A Potentiometric Study in 3.0 M $(Na)ClO_4$, Cl Media," *Acta Chem. Scand.*, **A31**, 705 (1977).

Smith, W. R., and R. W. Missen, *Chemical Reaction Equilibrium Analysis: Theory and Algorithms*, Wiley-Interscience, New York (1982).

Wagman, D. D., W. H. Evans, V. B. Parker, R. H. Schumm, I. Halow, S. M. Bailey, K. L. Churney, and R. L. Nuttal, "The NBS Tables of Chemical Thermodynamic Properties. Selected Values for Inorganic and C_1 and C_2 Organic Substances in SI Units," *J. Phys. Chem. Ref. Data*, **11**, Suppl. 2 (1982).

White, C. W., and W. D. Seider, "Computation of Phase and Chemical Equilibrium: IV," *AIChE J.*, **27**, 466 (1981).

Manuscript received Aug. 6, 1993, and revision received Oct. 25, 1993.

Correction

In the article titled "Concentric-Tube Airlift Reactors: Effects of Geometrical Design on Performance" by J. C. Merchuk, N. Ladwa, A. Cameron, M. Bulmer, and A. Pickett (July 1994, p. 1105), Eq. 15 should read as follows:

$$Eu' = 8.58\, Fr^{-1.51}\, Ga^{0.06}\, X_{dr}^{-1.1}\, M^{4.2} \qquad (15)$$